JACS
JOURNAL OF THE AMERICAN CHEMICAL SOCIETY
Article
pubs.acs.org/JACS

DNA Island Formation on Binary Block Copolymer Vesicles

Qingjie Luo,[†] Zheng Shi,[†] Yitao Zhang,[†] Xi-Jun Chen,[†] Seo-Yeon Han,[‡] Tobias Baumgart,[†] David M. Chenoweth,[†] and So-Jung Park*[,†,‡]

[†]Department of Chemistry, University of Pennsylvania, 231 South 34th Street, Philadelphia, Pennsylvania 19104, United States
[‡]Department of Chemistry and Nano Science, Ewha Womans University, Ewhayeodae-gil, Seodaemun-gu, Seoul 120-750, Korea

Supporting Information

ABSTRACT: Here, we report DNA-induced polymer segregation and DNA island formation in binary block copolymer assemblies. A DNA diblock copolymer of polymethyl acrylate-*block*-DNA (PMA-*b*-DNA) and a triblock copolymer of poly(butadiene)-*block*-poly(ethylene oxide)-*block*-DNA (PBD-*b*-PEO-*b*-DNA) were synthesized, and each was coassembled with a prototypical amphiphilic polymer of poly(butadiene)-*block*-poly(ethylene oxide) (PBD-*b*-PEO). The binary self-assembly of PMA-*b*-DNA and PBD-*b*-PEO resulted in giant polymersomes with DNA uniformly distributed in the hydrophilic PEO shell. When giant polymersomes were connected through specific DNA interactions, DNA block copolymers migrated to the junction area, forming DNA islands within polymersomes. These results indicate that DNA hybridization can induce effective lateral polymer segregation in mixed polymer assemblies. The polymer segregation and local DNA enrichment have important implications in DNA melting properties, as mixed block copolymer assemblies with low DNA block copolymer contents can still exhibit useful DNA melting properties that are characteristic of DNA nanostructures with high DNA density.

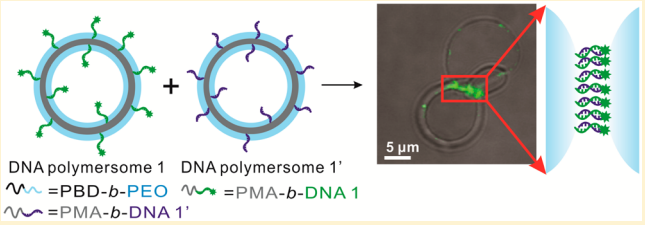

INTRODUCTION

Gold nanoparticles modified with a dense layer of oligonucleotides[1] have been extensively studied for many applications ranging from materials syntheses[2] to diagnostics and drug delivery.[3−7] The most attractive characteristic of DNA-modified gold particles is their unique DNA hybridization properties such as sharp melting transitions and high binding constants.[8] These unique properties originate from the cooperative interaction of densely packed DNA strands, and thus, they are independent of the core composition.[8] Therefore, researchers have developed ways to fabricate densely packed DNA nanostructures without the gold core.[9−12] Among them, DNA block copolymers are a particularly promising building block to fabricate such DNA nanostructures.[13−16] Assemblies of DNA block copolymers are composed of the polymer core and a high density DNA corona, and thus show similar DNA melting properties as DNA-modified gold particles mentioned above.[13] Moreover, functional molecules or nanoparticles can be readily incorporated into the polymer core of DNA block copolymer micelles.[12] Capitalizing on these attributes, researchers have actively studied DNA block copolymers for various applications including drug delivery[17,18] and gene therapy.[19−21] Lastly, the polymer strands composing the assemblies can undergo strand rearrangement and exchange, which allows for dynamic morphology changes in response to various external stimuli.[15]

An intriguing possibility arising from the strand rearrangement is the phase segregation and domain formation in mixed assemblies, which has not been previously investigated for DNA block copolymers. Phase segregation is a common phenomenon found in lipid bilayers composing cell membranes where different membrane components are segregated to form domains.[22] There is evidence indicating that such domain formation plays a critical role in many cellular functions such as signal transduction pathways, cell adhesion, cell migration, and synaptic transmission.[23]

Here, we fabricated giant vesicles from a DNA diblock copolymer of polymethyl acrylate-*block*-DNA (PMA-*b*-DNA) and a prototypical block copolymer of poly(butadiene)-*block*-poly(ethylene oxide) (PBD-*b*-PEO) (Scheme 1). We demonstrated that the two polymers composing the giant polymersomes undergo efficient polymer segregation upon the introduction of polymersomes containing complementary

Scheme 1. Binary Self-Assembly of PMA-*b*-DNA and PBD-*b*-PEO into Giant DNA Polymersomes

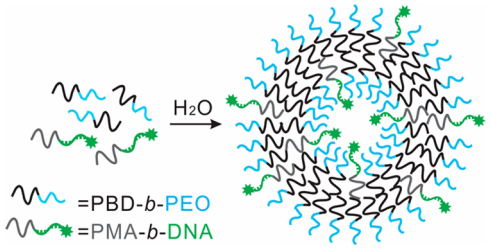

Received: April 21, 2016
Published: July 19, 2016

DOI: 10.1021/jacs.6b04076
J. Am. Chem. Soc. 2016, 138, 10157−10162

DNA. While such lateral segregation has been reported for lipids,[24−26] efficient DNA-induced segregation in polymer assemblies has remained elusive. Phase segregation in polymer assemblies is typically much slower than that in lipid bilayers due to the entanglement of high molecular weight polymers,[27,28] and thus the segregation behavior can be quite different in the two systems. The DNA-induced polymer segregation shown here generates high density DNA domains on vesicle surfaces, which allows for cooperative DNA binding even at low DNA block copolymer contents. To the best of our knowledge, this report is the first to show the efficient DNA-induced segregation in polymer assemblies, and to demonstrate how the phase behavior influences the molecular recognition properties of DNA. The stability and chemical diversity of polymers together with the DNA segregation observed here open up new possibilities in polymeric DNA nanostructures.

RESULTS AND DISCUSSION

Synthesis and Characterization of PMA-*b*-DNA. An amphiphilic DNA block copolymer, PMA-*b*-DNA was synthesized through the coupling of carboxylic-acid-terminated polymethyl acrylate (PMA, Mn = 7800 kg mol^{-1}) to 5′-amine-modified 25 base oligonucleotide strands (DNA 1:5′-A10-ATCCTTATCAATATT-FAM-3′) attached on solid supports (Figure 1a).[21] A green fluorescent dye (6-FAM) was

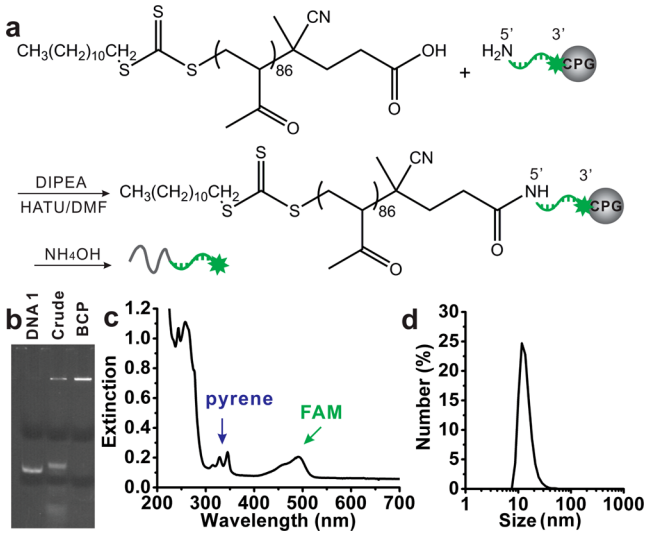

Figure 1. (a) Synthetic schemes for PMA-*b*-DNA. (b) PAGE analyses (lane 1, DNA 1; lane 2, crude product containing PMA-*b*-DNA and unbound DNA strands; lane 3, purified PMA-*b*-DNA). (c) Extinction spectrum of purified PMA-*b*-DNA in water. (d) DLS data of purified PMA-*b*-DNA micelles in water.

attached at the 3′ end of DNA to monitor the presence of DNA. Typically, pyrene acrylate dyes were incorporated into PMA at a ratio of one pyrene molecule per polymer chain to track the presence of PMA (Supporting Information). Gel electrophoresis data show that DNA block copolymers were successfully synthesized and purified from the crude product of DNA block copolymers (Figure 1b); as DNA block copolymers form nanoscale assemblies in water, they remain in the loading well, while unconjugated free DNA strands move along the electric field. The successful conjugation was also confirmed by the coexistence of the fingerprint-like absorption peaks of pyrene and the absorption peak of FAM at 494 nm as well as the DNA peak at 260 nm (Figure 1c). On the basis of the absorbance at 494 nm of 6-FAM and 335 nm of pyrene, the molar ratio of the two dye molecules was calculated to be 0.88:1, which is close to the predesigned 1:1 ratio. Due to the amphiphilic nature, PMA-*b*-DNA spontaneously forms micelles in water after gel purification. The diameter of the polymer micelles was determined to be 14 nm by dynamic light scattering (DLS) (Figure 1d).

Fabrication of Giant Polymersomes from PMA-*b*-DNA and PBD-*b*-PEO (DNA Polymersome). Giant DNA polymersomes were prepared by the film hydration of PMA-*b*-DNA and PBD-*b*-PEO (Scheme 1). PBD-*b*-PEO diblock copolymers can self-assemble into various structures, such as spherical micelles, bilayers, and cylindrical micelles in water, depending on the relative block ratio.[29] In this study, PBD_{52}-*b*-PEO_{32} with the PEO weight fraction (w_{PEO}) of 0.33 was used for the binary self-assembly, as PBD_{52}-*b*-PEO_{32} readily forms giant vesicles by a film hydration method (Figure S6a). In typical experiments, PMA-*b*-DNA and PBD_{52}-*b*-PEO_{32} were mixed at a molar ratio of 1:1600 in a $CHCl_3$/DMSO mixture (5$CHCl_3$/1DMSO). The solution (60 μL) was placed on the bottom of a glass vial and dried by a stream of N_2 gas, which generated a thin film of mixed polymers on the bottom of the vial. The film was further dried under vacuum overnight, and then hydrated in 500 μL of 0.1 M phosphate buffered saline (PBS) solution (100 mM NaCl, 10 mM phosphate, pH = 7.17). The 12 h incubation in the buffer produced suspensions of giant vesicles of the two polymers.

Figure 2a,b presents confocal microscope images (see Figure S6b for more images) of giant polymersomes formed with

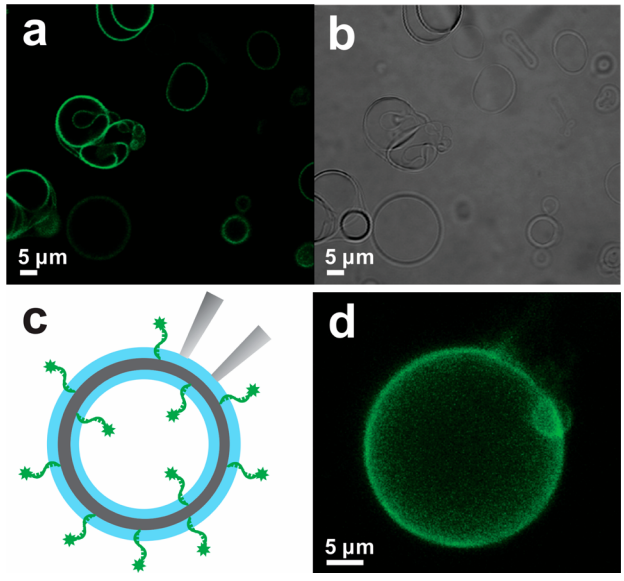

Figure 2. (a, b) Confocal laser scanning fluorescence (a) and transmission (b) images of giant DNA polymersomes formed from PBD_{52}-*b*-PEO_{32} and PMA-*b*-DNA. (c) A pictorial description of a DNA polymersome immobilized onto a micropipette. (d) A Z-stack image of a DNA giant polymersome.

0.062% DNA block copolymer, showing well-defined giant vesicles composed of the hydrophobic inner layer of PBD and PMA and the hydrophilic corona of PEO and DNA (Scheme 1). Green fluorescence from vesicles indicates that DNA block copolymers are incorporated into the vesicle membranes. Z-stack images of giant polymersomes obtained by immobilizing

DOI: 10.1021/jacs.6b04076
J. Am. Chem. Soc. 2016, 138, 10157−10162

Scheme 2. Schematic Description of DNA-Induced Self-Assembly of DNA Polymersomes and the Formation of DNA Islands at the Junction Sites

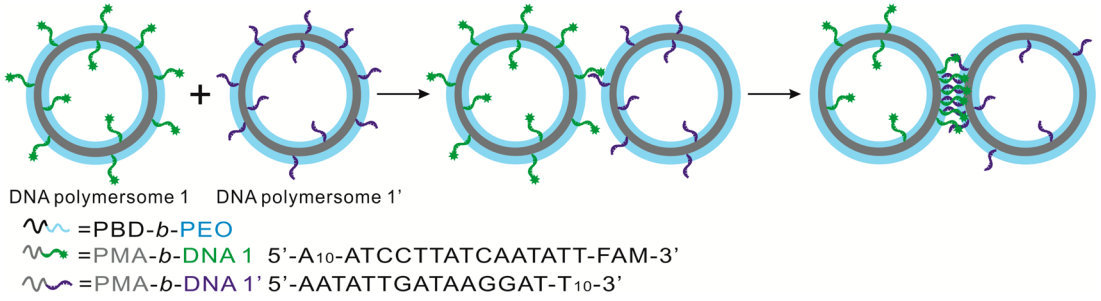

them onto a micropipette (Figure 2c) show uniform distribution of FAM-labeled DNA on the polymersome surface (Figure 2d).

Two sets of giant DNA polymersomes (polymersome 1 and polymersome 1′) were prepared using complementary DNA strands, DNA 1 and DNA 1′ (Scheme 2). The two sets of giant DNA polymersomes were mixed together in 0.1 M PBS buffer to induce the hybridization of DNA 1 and DNA 1′ and consequently the aggregation of polymersomes (Scheme 2). Optical microscope images taken after 16 h incubation showed polymersome aggregates as expected (Figure 3a and Figures S8a,b and S9). In our control experiment where polymersomes 1 and 1′ were mixed in water, there was no obvious aggregation (Figure S10a,b). To further confirm the duplex formation at the junction, ethidium bromide, which is a commonly used reagent to visualize DNA duplexes, was introduced to polymersome aggregates. The orange fluorescence observed at the junction area (Figure 3b, and Figure S8c,d) confirms that the polymersome aggregates were formed through specific DNA interactions.

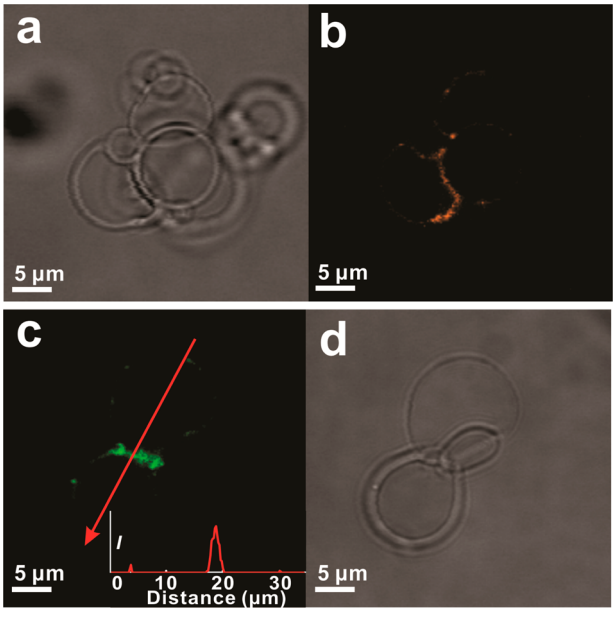

Figure 3. (a, b) Transmission (a) and fluorescence (b) images of polymersome aggregates incubated with ethidium bromide. (c, d) Confocal laser scanning fluorescence (c) and transmission (d) images of polymersome aggregates. A fluorescence intensity line profile is shown in the inset of part c.

Interestingly, fluorescent microscope images reveal that FAM fluorescence from DNA is also localized at the junction between polymersomes (Figure 3c,d and Figure S8a,b). This result indicates that polymer strands in the giant vesicles are mobile and DNA block copolymers accumulate at the junction area, creating DNA islands on polymersome surfaces. Fluorescence recovery after photobleaching (FRAP) measurements shows that DNA block copolymers in mixed polymersomes have lateral diffusivity (Figure S7), which is consistent with the observation of DNA-rich island formation. The size of DNA islands should mainly depend on the number of junctions per vesicles, and the diameter of the island ranged from submicrometers to a few micrometers.

The DNA-induced lateral segregation of polymers in this study occurred with overnight incubation, which is relatively fast, compared to previously studied phase segregation in polymersomes.[27,28] Phase segregation in polymersomes is known to be much slower than in lipid bilayers[24,25,30] due to the entanglement of large molecular weight polymers. For example, Discher and co-workers reported that micrometer-sized polymersomes made of PBD-*b*-PEO and poly(butadiene)-*block*-poly(acrylic acid) (PBD-*b*-PAA) showed fully segregated polymer domains after 40 h incubation with the addition of cross-bridging polyvalent cations.[27] In another example, nanometer-sized polymersomes made of PBD-*b*-PEO and poly(2-(diisopropylamino)ethyl methacrylate)-*block*-poly((2-methacryloyloxy)ethyl phosphorylcholine) (PDPA-*b*-PMPC) showed the evolution of surface patterns of phase segregation over the time-scale of more than a month.[28] We attribute the relatively efficient polymer separation in mixed polymersomes observed here to the driving force of forming multiple DNA linkages between polymersomes.

Preparation and Assembly of PBD-*b*-PEO-*b*-DNA Triblock Copolymers. The DNA island formation shown in Figure 3a is advantageous, as it indicates that the useful DNA binding properties of DNA block copolymer micelles[8] might occur in the mixed assemblies with low DNA content. To examine how the polymer segregation affects DNA binding properties, we prepared a new set of mixed assemblies from a DNA triblock copolymer of poly(butadiene)-*block*-poly(ethylene oxide)-*block*-DNA (PBD-*b*-PEO-*b*-DNA) (Scheme 3). This new design allows for the formation of binary assemblies where DNA strands are not buried inside the PEG layer, which can potentially destabilize DNA duplexes.[31]

The DNA triblock copolymer, PBD-*b*-PEO-*b*-DNA, was synthesized with DNA 2 (5′-ATCCTTATCAATATT-FAM-3′) and PBD-*b*-PEO (Mn, 3800 kg mol^{-1}; w_{PEO}, 0.34), following the same procedure used for DNA diblock copolymers (see Supporting Information for details). The

DOI: 10.1021/jacs.6b04076
J. Am. Chem. Soc. 2016, 138, 10157−10162

Scheme 3. Binary Self-Assembly of PBD-*b*-PEO and PBD-*b*-PEO-*b*-DNA into Small Micelles[a]

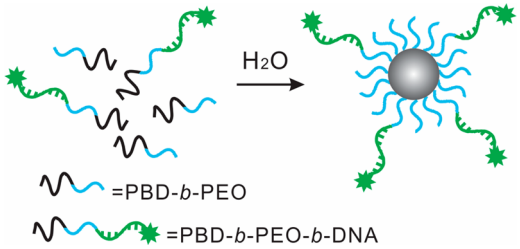

[a]The grey sphere represents the PBD core of a micelle.

synthesized polymers were purified by gel electrophoresis (Figure 4a). The purified DNA triblock copolymers showed distinct DNA absorption peak at 260 nm and 6-FAM peak at 480 nm (Figure 4b).

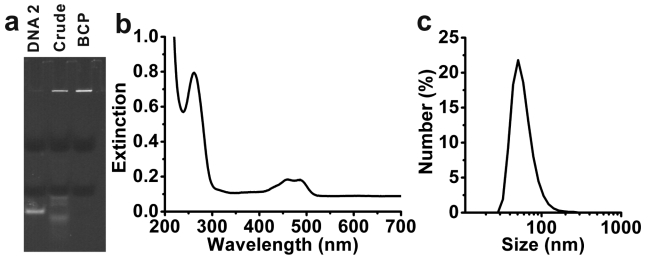

Figure 4. (a) PAGE analysis of synthesized triblock copolymers (lane 1, DNA 2; lane 2, crude product containing PBD-*b*-PEO-*b*-DNA and unbounded DNA 2; lane 3, purified PBD-*b*-PEO-*b*-DNA). (b) Extinction spectrum of purified PBD-*b*-PEO-*b*-DNA in water. (c) DLS data of PBD-*b*-PEO-*b*-DNA micelles prepared by film hydration and subsequent membrane extrusion.

To prepare binary assemblies, PBD-*b*-PEO-*b*-DNA was mixed with PBD_{46}-*b*-PEO_{30} at varying molar ratios (100 mol %, 50 mol %, 10 mol % of PBD-*b*-PEO-*b*-DNA) in a small amount of $CHCl_3$/DMSO mixture ($4CHCl_3$:1DMSO, 50 μL). Suspensions of binary polymer assemblies were prepared following the procedure described above for diblock copolymers. The polymer suspensions were extruded through a polycarbonate membrane filter with 400 nm pores to obtain uniform nanoscale assemblies for DNA melting studies. Transmission electron microscopy (TEM) images showed that small spherical assemblies were formed by the procedure (Figure S11a,b). The diameters of the assemblies were determined to be 62, 63, and 65 nm for 100%, 50%, 10% samples, respectively, by DLS (Figure S11c–e).

Another DNA triblock copolymer, polystyrene-*block*-poly(ethylene oxide)-*block*-DNA (PS-*b*-PEO-*b*-DNA, Mn, 7000 kg mol^{-1}; w_{PEO}, 0.29), and their assemblies were also prepared by the same procedure as PBD-*b*-PEO-*b*-DNA to investigate the effect of the core polymer (see Supporting Information for synthesis and characterization data, Figures S4 and S12).

DNA Melting Properties of Binary Assemblies. To investigate the melting properties of binary assemblies, PBD-*b*-PEO-*b*-DNA triblock copolymer assemblies were mixed with gold nanoparticles modified with DNA 2′ (5′-A_{10}-AATATTGATAAGGAT-3′) in 0.1 M PBS buffer, as illustrated in Figure 5a. The mixture was then incubated at 50 °C for 16 h to facilitate the polymer strand migration and DNA duplex formation. DNA hybridization connected nanoparticles and

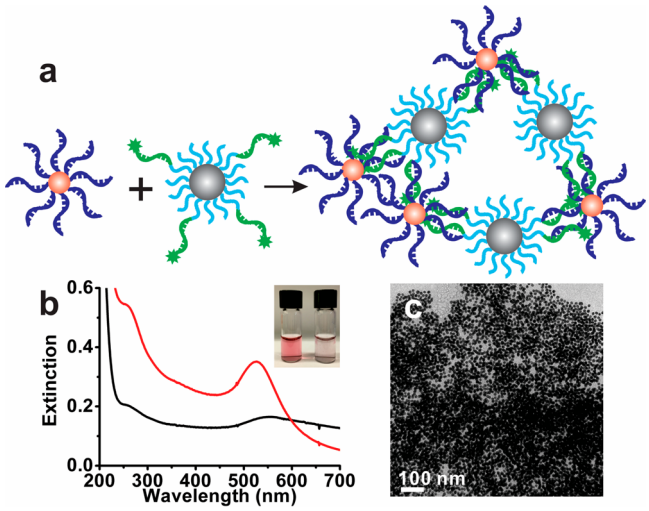

Figure 5. (a) Schematic description of DNA-induced self-assembly of DNA triblock copolymer micelles and DNA-modified gold nanoparticles. (b) Extinction spectra of dispersed gold nanoparticles (red line) and gold nanoparticle aggregates cross-linked by polymer assemblies (black line). A picture of dispersed nanoparticles (left) and nanoparticle aggregates (right) is shown in the inset. (c) A TEM image of nanoparticle networks.

polymer assemblies together into macroscopic aggregates (Figure 5b,c). The assembly process caused an expected red-shift and broadening of the 520 nm (SPR) band of gold nanoparticles and the corresponding red to purple color change (Figure 5b).

Melting curves were obtained by monitoring the extinction of gold nanoparticles at 520 nm (Figure 6). A sharp melting transition was observed for the assemblies made of 100 mol % PBD-*b*-PEO-*b*-DNA triblock copolymer (fwhm: 1.9 °C), as expected, due to the cooperative interaction of densely packed DNA strands (Figure 6a and Figure S15a).[13] Melting curves from binary assemblies containing 50 mol % PBD-*b*-PEO-*b*-

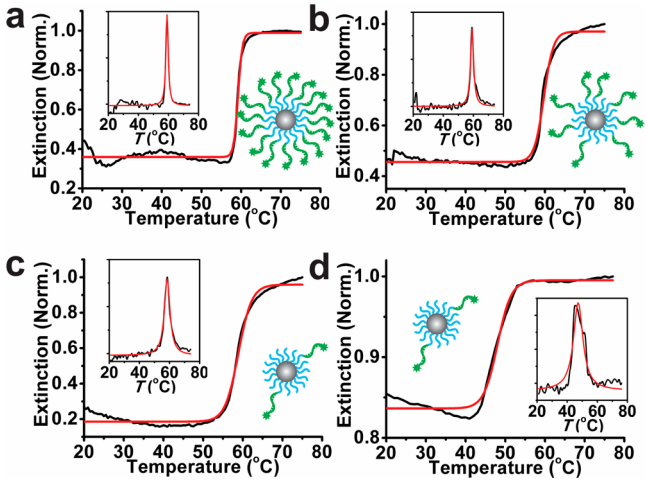

Figure 6. DNA melting transitions of aggregates formed from DNA-modified gold nanoparticles and binary micelles with (a) 100 mol %, (b) 50 mol %, and (c) 10 mol % DNA triblock copolymer (PBD-*b*-PEO-*b*-DNA) content, and (d) 10 mol % PS-*b*-PEO-*b*-DNA, obtained by monitoring the extinction at 520 nm. The insets show the first derivatives of the melting curves. The black and the red curves are experimental data and fitted curves, respectively.

DOI: 10.1021/jacs.6b04076
J. Am. Chem. Soc. 2016, 138, 10157–10162

DNA (Figure 6b and Figure S15b) and 10 mol % DNA block copolymers (Figure 6c and Figure S15c) showed slight broadening with fwhm values of 2.4 and 4.1 °C, respectively. However, they still remain much sharper than that of plain dsDNA (fwhm: 9.8 °C, Figure S16a,b). The melting curves measured without the thermal annealing process showed fwhm of 2.2, 2.8, and 6.7 °C for 100%, 50%, and 10% samples, respectively (Figure S13), showing that the annealing process causes sharpening of the melting transition for low DNA content assemblies.

To further investigate the effect of polymer segregation on melting behaviors, the same set of assemblies was prepared from PS-*b*-PEO-*b*-DNA and PS-*b*-PEO containing a high glass temperature (100 °C)[32] polymer, PS. Figure 6d presents the melting curve of the binary assembly containing 10% PS-*b*-PEO-*b*-DNA, which indeed shows broader melting transition (fwhm: 7.7 °C) and lower melting temperature (45.3 °C) than the assemblies with PBD core (Figure 6c) (see Figure S14 for more melting data). The fwhm values and melting temperatures of mixed assemblies are summarized in Table 1.

Table 1. FWHM/Melting Temperatures for Mixed Assemblies with Different DNA Block Copolymer Contents

DNA content	PBD-*b*-PEO-*b*-DNA	PS-*b*-PEO-*b*-DNA
100%	1.9 °C/59.1 °C	1.8 °C/56.2 °C
50%	2.4 °C/59.1 °C	2.0 °C/56.3 °C
10%	4.1 °C/58.4 °C	7.7 °C/45.3 °C

These results support our hypothesis that the polymer segregation (Figure 3) leads to cooperative DNA binding and sharp melting transitions of DNA in mixed assemblies. Unlike DNA affixed on nanoparticle surface by covalent bonds, DNA block copolymers can diffuse laterally as long as the T_g of the core polymer is sufficiently low. In the assemblies made of PS, the polymer strand migration should be much slower than those made of PBD, and therefore, the melting transition becomes significantly broader as the DNA block copolymer content is reduced. On the other hand, for nonglassy polymers, DNA block copolymers can form locally concentrated DNA islands at the binding sites, which allows for cooperative binding even at low DNA contents.

CONCLUSIONS

In summary, we have fabricated binary assemblies of DNA block copolymers (i.e., PMA-*b*-DNA, PBD-*b*-PEO-*b*-DNA) and a prototypical block copolymer of PBD-*b*-PEO. Binary self-assembly of PBD-*b*-PEO and PMA-*b*-DNA at low DNA block copolymer content adopts the morphology of PBD-*b*-PEO and forms giant polymersomes, where DNA block copolymers are uniformly distributed in the membrane. Note that DNA block copolymer alone typically forms small micelles in water due to the highly charged DNA backbone.[33] Mixed assembly reported here provides a way to form various types of DNA block copolymer assemblies that are difficult to make on their own. Interestingly, when the giant polymersomes with complementary DNA strands were mixed together to induce aggregation of polymersomes, DNA block copolymers segregated to the binding area, forming DNA islands at the junction between polymersomes. The efficient accumulation of DNA block copolymers at the junction observed here compared to the typical phase segregation in polymersomes was attributed to the driving force of forming multiple DNA linkages between polymersomes. This polymer segregation has important consequences in DNA melting properties of mixed assemblies. Binary micelles formed from DNA triblock copolymer of PBD-*b*-PEO-*b*-DNA and PBD-*b*-PEO at varying DNA triblock copolymer contents showed that the unique sharp melting transition of DNA block copolymer micelles is maintained in micelles with low DNA block copolymer contents (i.e., 50%, 10%). The type of hydrophobic polymer affected the melting behavior of binary assemblies. The assemblies made from PS-*b*-PEO-*b*-DNA and PS-*b*-PEO, which contains a glassy PS core, showed broader melting transitions at low DNA block copolymer contents. This result supports that the segregation of DNA block copolymers affects their DNA melting properties. Note that it is advantageous to use low DNA block copolymer content in forming DNA-decorated polymer nanostructures, as DNA block copolymers are more costly to make than the matrix amphiphilic polymers. We believe that this work is the first to demonstrate the efficient DNA-induced polymer segregation in mixed assemblies and to show how it affects the DNA melting properties. The findings of this study demonstrate that the binary assemblies of DNA block copolymers and other commonly used amphiphilic polymers provide an opportunity to form various types of assembly structures that are difficult to make from DNA block copolymer by itself without losing its excellent DNA hybridization properties.

EXPERIMENTAL SECTION

Synthesis of PMA-*b*-DNA. PMA-*b*-DNA was synthesized by coupling carboxylate-terminated PMA and amine-modified oligonucleotides. PMA was synthesized by RAFT polymerization. See Supporting Information for its complete synthetic procedure and characterization data. For DNA coupling, purified PMA (0.264 g, 34 μmol) was dissolved in 500 μL of anhydrous DMF. Then, *N*,*N*-diisopropylethylamine (48 μL, 280 μmol) and 1-[bis(dimethylamino)-methylene]-1*H*-1,2,3-triazolo[4,5-*b*]pyridinium 3-oxid hexafluorophosphate (HATU) (13 mg, 34 μmol) were subsequently added to the solution.[21] The mixture was vortexed for 10 min to preactivate the coupling reaction. Then, 5′-amino-modified DNA on CPG beads solid support (ca. 1 μmol, MMT deprotected) was added to the solution. The mixture was kept on a shaker at room temperature overnight. The CPG beads were then washed with ∼200 mL of DMF to remove unbound PMA homopolymers. The DNA block copolymer strands were cleaved from the CPG beads by incubating them in ∼1 mL of concentrated ammonia at 65 °C for 2 h. After 2 h of reaction, ammonia was evaporated by loosening the vial cap. The CPG beads were filtered and subsequently washed with about 4 mL of water. DNA block copolymers and unbound single strand DNAs were collected and separated by PAGE gel electrophoresis.

Fabrication of Giant Polymersomes. Giant polymersomes were prepared by the film hydration method. First, 50 μL of PBD_{52}-*b*-PEO_{32} solution ($CHCl_3$, 4 mg/mL) was mixed with 10 μL of PMA-*b*-DNA solution (DMSO, 3 μM). The mixture was dried under the nitrogen gas flow in the bottom of a glass vial, and then the dried polymer mixture was kept under vacuum for >6 h to ensure that the solvents were completely removed. Finally, 500 μL of 0.1 M PBS buffer (100 mM NaCl, 10 mM phosphate buffer pH = 7.17) was added to the film and heated at 50 °C for 12 h to form mixed giant polymersomes. For optical imaging, 5 μL of the polymersome solution was placed into the glass bottom of a cell culture dish.

Fabrication of Small Micelles. Mixed small micelles were prepared by passing the assemblies formed by the above-described film hydration method through the membrane extrusion filter. Typically, 100 μL of PBD-*b*-PEO-*b*-DNA (DMSO, 4 μM) solution was mixed with 35 μL of PBD_{46}-*b*-PEO_{30} solution ($CHCl_3$, 0.4 mg/mL) for mixed assemblies with 10 mol % DNA block copolymer content or with 38 μL of PBD_{46}-*b*-PEO_{30} solution ($CHCl_3$, 0.04 mg/

DOI: 10.1021/jacs.6b04076
J. Am. Chem. Soc. 2016, 138, 10157−10162

mL) for mixed assemblies with 50 mol % DNA block copolymer contents. For PS-*b*-PEO-*b*-DNA assemblies, 133 μL of PS-*b*-PEO-*b*-DNA (DMSO, 3 μM) solution was mixed with 35 μL of PS_{48}-*b*-PEO_{46} solution ($CHCl_3$, 0.74 mg/mL) or 38 μL of PS_{48}-*b*-PEO_{46} ($CHCl_3$, 0.074 mg/mL) solution for binary assemblies containing 10 mol % or 50% DNA block copolymers, respectively. The mixture was placed into a glass vial, and the solvent was evaporated under vacuum for at least 6 h. Then, 100 μL of 0.1 M PBS buffer (100 mM NaCl, 10 mM phosphate buffer pH = 7.17) was added to the polymer film in the vial. The solution was vortexed, frozen, and thawed 5 times before the extrusion. Finally, the samples were extruded 38 times through Whatman Nucleopore tracketch membrane with a pore size of 400 nm.

DNA-Induced Aggregation of Giant Polymersomes. In a typical experiment, 100 μL of each polymersome solution was placed in a microcentrifuge tube. The mixture was incubated at 55 °C for 5 min, and then allowed to cool down to room temperature overnight prior to the optical imaging.

■ ASSOCIATED CONTENT

Supporting Information

The Supporting Information is available free of charge on the ACS Publications website at DOI: 10.1021/jacs.6b04076.

Detailed experimental procedures and characterization data, additional confocal images of polymer vesicles, additional characterization data of binary assemblies, and additional UV−vis DNA melting data of binary assemblies (PDF)

■ AUTHOR INFORMATION

Corresponding Author

*sojungpark@ewha.ac.kr

Notes

The authors declare no competing financial interest.

■ ACKNOWLEDGMENTS

S.-J.P. acknowledges the financial support from the National Research Foundation of Korea grant funded by the Korea government (MSIP) (NRF-2015R1A2A2A01003528) and the Camille Dreyfus Teacher−Scholar Award. The authors thank Dr. Dewight R. Williams for help with cryo-TEM imaging.

■ REFERENCES

(1) Mirkin, C. A.; Letsinger, R. L.; Mucic, R. C.; Storhoff, J. J. *Nature* **1996**, *382*, 607−609.
(2) Estephan, Z. G.; Qian, Z.; Lee, D.; Crocker, J. C.; Park, S.-J. *Nano Lett.* **2013**, *13*, 4449−4455.
(3) Chan, W. C. W.; Nie, S. *Science* **1998**, *281*, 2016−2018.
(4) Rosi, N. L.; Mirkin, C. A. *Chem. Rev.* **2005**, *105*, 1547−1562.
(5) De, M.; Ghosh, P. S.; Rotello, V. M. *Adv. Mater.* **2008**, *20*, 4225−4241.
(6) Lee, K.; Drachev, V. P.; Irudayaraj, J. *ACS Nano* **2011**, *5*, 2109−2117.
(7) de Vries, J. W.; Zhang, F.; Herrmann, A. *J. Controlled Release* **2013**, *172*, 467−483.
(8) Jin, R.; Wu, G.; Li, Z.; Mirkin, C. A.; Schatz, G. C. *J. Am. Chem. Soc.* **2003**, *125*, 1643−1654.
(9) Cutler, J. I.; Auyeung, E.; Mirkin, C. A. *J. Am. Chem. Soc.* **2012**, *134*, 1376−1391.
(10) Banga, R. J.; Chernyak, N.; Narayan, S. P.; Nguyen, S. T.; Mirkin, C. A. *J. Am. Chem. Soc.* **2014**, *136*, 9866−9869.
(11) Cutler, J. I.; Zhang, K.; Zheng, D.; Auyeung, E.; Prigodich, A. E.; Mirkin, C. A. *J. Am. Chem. Soc.* **2011**, *133*, 9254−9257.
(12) Chen, X.-J.; Sanchez-Gaytan, B. L.; Hayik, S. E. N.; Fryd, M.; Wayland, B. B.; Park, S.-J. *Small* **2010**, *6*, 2256−2260.
(13) Li, Z.; Zhang, Y.; Fullhart, P.; Mirkin, C. A. *Nano Lett.* **2004**, *4*, 1055−1058.
(14) Cottenye, N.; Syga, M.-I.; Nosov, S.; Muller, A. H. E.; Ploux, L.; Vebert-Nardin, C. *Chem. Commun.* **2012**, *48*, 2615−2617.
(15) Chien, M.-P.; Rush, A. M.; Thompson, M. P.; Gianneschi, N. C. *Angew. Chem., Int. Ed.* **2010**, *49*, 5076−5080.
(16) Albert, S. K.; Thelu, H. V. P.; Golla, M.; Krishnan, N.; Chaudhary, S.; Varghese, R. *Angew. Chem., Int. Ed.* **2014**, *53*, 8352−8357.
(17) Alemdaroglu, F. E.; Alemdaroglu, N. C.; Langguth, P.; Herrmann, A. *Adv. Mater.* **2008**, *20*, 899−902.
(18) Schnitzler, T.; Herrmann, A. *Acc. Chem. Res.* **2012**, *45*, 1419−1430.
(19) Liu, H.; Zhu, Z.; Kang, H.; Wu, Y.; Sefan, K.; Tan, W. *Chem. - Eur. J.* **2010**, *16*, 3791−3797.
(20) Kwak, M.; Musser, A. J.; Lee, J.; Herrmann, A. *Chem. Commun.* **2010**, *46*, 4935−4937.
(21) Rush, A. M.; Thompson, M. P.; Tatro, E. T.; Gianneschi, N. C. *ACS Nano* **2013**, *7*, 1379−1387.
(22) Pike, L. J. J. *J. Lipid Res.* **2006**, *47*, 1597−1598.
(23) Munro, S. *Cell* **2003**, *115*, 377−388.
(24) Hadorn, M.; Eggenberger Hotz, P. *PLoS One* **2010**, *5*, e9886.
(25) Beales, P. A.; Nam, J.; Vanderlick, T. K. *Soft Matter* **2011**, *7*, 1747−1755.
(26) Heberle, F. A.; Feigenson, G. W. *Cold Spring Harbor Perspectives in Biology*; 2011, Vol. 3.
(27) Christian, D. A.; Tian, A.; Ellenbroek, W. G.; Levental, I.; Rajagopal, K.; Janmey, P. A.; Liu, A. J.; Baumgart, T.; Discher, D. E. *Nat. Mater.* **2009**, *8*, 843−849.
(28) LoPresti, C.; Massignani, M.; Fernyhough, C.; Blanazs, A.; Ryan, A. J.; Madsen, J.; Warren, N. J.; Armes, S. P.; Lewis, A. L.; Chirasatitsin, S.; Engler, A. J.; Battaglia, G. *ACS Nano* **2011**, *5*, 1775−1784.
(29) Jain, S.; Bates, F. S. *Science* **2003**, *300*, 460−464.
(30) Veatch, S. L.; Keller, S. L. *Biophys. J.* **2003**, *85*, 3074−3083.
(31) Knowles, D. B.; LaCroix, A. S.; Deines, N. F.; Shkel, I.; Record, M. T. *Proc. Natl. Acad. Sci. U. S. A.* **2011**, *108*, 12699−12704.
(32) *Physical Properties of Polymers Handbook*; Mark, J. E., Ed.; AIP Press: Woodbury, NY, 1996.
(33) Fuks, G.; Mayap Talom, R.; Gauffre, F. *Chem. Soc. Rev.* **2011**, *40*, 2475−2493.

DOI: 10.1021/jacs.6b04076
J. Am. Chem. Soc. 2016, 138, 10157−10162